[Original]

A Basic Study to Clarify the Porcelain-Metal Bonding Mechanism
— Analysis of the Oxidized Surface of Gold Alloys by Reflection Electron Diffraction —

Hiroki OHNO, Yasuo KANZAWA, Isao KAWASHIMA, Yuro YAMANE, and Shoko TAKANOHASHI

Department of Dental Materials Science, School of Dentistry, HIGASHI-NIPPON-GAKUEN UNIVERSITY

(Chief : Prof. Yasuo KANZAWA)

Abstract

The oxide in contact with porcelain, the top layer of the oxidized surface of an alloy, is of critical importance when considering the reaction at the interface between porcelain and alloy. The present study uses Reflection High Energy Electron Diffraction to obtain detailed knowledge of the oxidized surface of gold alloys containing small amounts of In and Sn (total 1.5wt %), oxidized at 1000 ℃ in air for 30 sec to 60 min.

The oxidized alloy surface is not always covered with a uniform oxide layer, in the case of alloys containing both In and Sn, or In alone, the alloy itself is partially exposed. The roughness of the oxidized surface due to high temperature oxidation increases with increasing oxidation times. In_2O_3, rather than SnO_2, is preferentially formed when the Sn content is less than 0.6 wt% at short oxidation times, SnO_2 can not be detected by the reflection electron diffraction.

Key words : Porcelain, gold alloy, oxidation, electron diffraction

Introduction

The mechanism of porcelain-metal bonding has been investigated in simplified systems of silica glass and gold-indium binary alloys by Electron Spectroscopy for Chemical Analysis(ESCA).[1] However, the bonding mechanism in porcelains and alloys for dental use has not been satisfactorily clarified.[2~6] This is caused by the complicated composition of both the porcelain and alloy, and the submicrometer thickness of the reaction layer.[7,8] Further basic research is necessary to elucidate the bonding mechanism.

Small amounts, up to 1.5 wt%, of base metals such as In, Sn, Ni, and Fe in commercial gold alloys for porcelain-metal bonding have been shown to oxidize selectively during the high temperature cycles used for pre-heating(degassing)of alloy and firing of porcelain.[9] It has become clear that oxides formed on the alloy surface are necessary to obtain good bonding strength. However, the role of these oxides in the bonding mechanism is not clear.

We have reported the structure and composition of the oxidation zone on alloys using various experimental techniques, including scanning electron microscopy, electron probe X-ray micro-analysis, and X-ray diffraction.[10] This study uses Reflection High Energy Electron Diffraction to obtain a detailed knowledge of the oxidized surface of gold alloys containing small amounts of In and Sn. Scattering of electrons by atoms is much greater (10^4 times) than scattering of X-rays,[11] and electron diffraction reveals the crystal structure of a very thin layer from a few tens of Å to several hundred Å, compared with the 0.01 μm to 100 μm obtained with X-ray diffraction. Therefore, electron diffraction is a very useful method in the analysis of the top layer of the oxidized alloy surface which reacts with the fused porcelain.

Materials and Methods

Table 1 shows the compositions of the gold alloys used in the experiments. The alloys contained Au, Pt, Pd, and Ag as noble metals, and In and Sn as the base metals. The In and Sn content in the alloys totaled 1.5 wt% and the respective amounts were varied in 0.3 wt% increments in the 0-1.5 wt% range. All metals used were of a purity better than 99.9 %. The metals were weighed to give 10 g samples, and prepared by melting in an argon gas atmosphere. The melting was done in an alumina crucible covered with graphite using a high frequency induction furnace. Weight loss during melting was less than 0.02%.

The alloys were cast in 9 mm$^{\phi}$ x 0.5 mm ingots by a centrifugal casting machine (Jelenko, Thermotrol-2500) to prepare specimens for the reflection electron diffraction. The specimens were polished metallographically and then oxidized by heating in an electric furnace at 1000 ℃ in air for 30 sec, 1 min, 5 min, 20 min, and 60 min.

Reflection high energy electron diffraction patterns were taken using an electron microscope (Hitachi, H-500) with an accelerating voltage of 100 kV. The camera constant was calibrated taking the transmission diffraction pattern of a gold film immediately before and after taking the reflection patterns. The diameter of the diffraction ring measured on the film (Fuji, FG for an electron microscope) enlarged the diffraction pattern.

In order to compare the results of electron diffraction and X-ray diffraction, plate specimens were subjected to X-ray diffraction with a diffractometer (Rigaku Denki Geigerflex, 2013) under

Table 1. Compositions of the gold alloys in wt%.

No.	Au	Pt	Pd	Ag	In	Sn
1	85.5	6	6	1	1.50	—
2					1.20	0.30
3					0.90	0.60
4					0.60	0.90
5					0.30	1.20
6					—	1.50

Cu Kα radiation with a Ni filter. The substances on the alloy surface were identified from the ASTM card-index on the basis of the measured spacings for both the electron and X-ray diffraction.

Lattice parameters of unoxidized alloys were determined by a Debye-Scherrer camera using annealed fine powdered specimens passing through a 300 mesh sieve.

Topographical changes on the oxidized surface with oxidation times were observed by an electron probe microanalyzer (Shimadzu, EMX-SM) using the same specimens as for electron diffraction.

Results

Figure 1 shows a reflection high energy electron diffraction pattern obtained from the surface of Alloy No.1 oxidized for 60 min. In Table 2, the observed lattice spacings and intensities of the diffraction rings are shown and compared with the lattice spacings of the alloy measured by the Debye-Scherrer method and data for In_2O_3 from the ASTM card-index. A comparison with the reference substances measured by X-rays shows that diffraction is from both the alloy matrix and In_2O_3 : Diffraction from the alloy matrix is identified from the 200 reflection of the matrix, as the 111 reflection of the matrix overlaps with the 411 reflection of In_2O_3. This shows that the alloy surface is not covered with a uniform In_2O_3 film.

Figure 2 shows a reflection electron diffraction pattern obtained from Alloy No.3 oxidized for 5 min. The diffraction rings are smooth and sharp in contrast to the spotty rings with the long oxidation time shown in Fig.1. Table 3 shows the observed lattice spacings and intensities of the diffraction rings with data for reference substances. Though Alloy No.3 contains 0.6 wt % Sn, the diffraction rings are from the alloy matrix and In_2O_3, not from SnO_2.

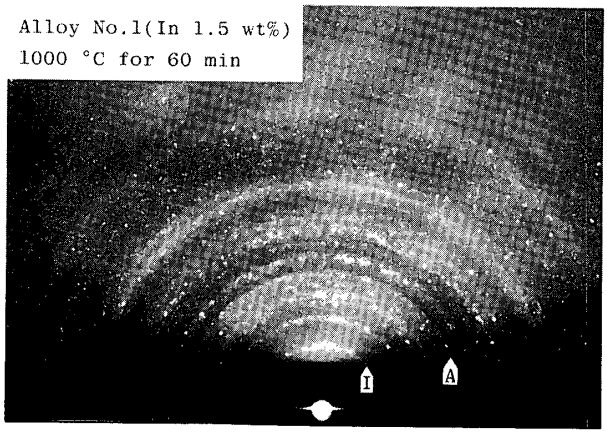

Fig. 1 Reflection high energy electron diffraction pattern from the surface of Alloy No.1, oxidized for 60 min. A : 200 reflection of alloy matrix, I : 211 reflection of In_2O_3.

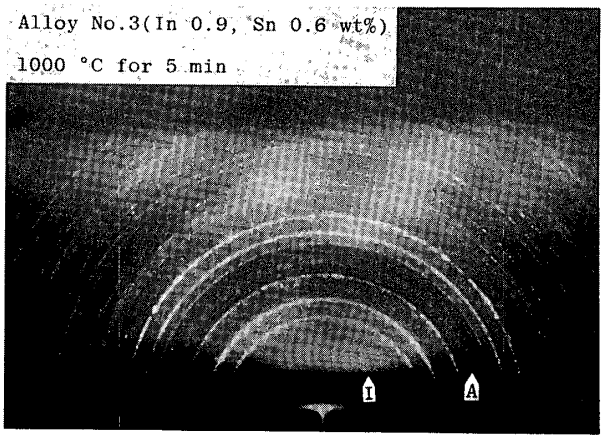

Fig. 2 Reflection high energy electron diffraction pattern from the surface of Alloy No.3, oxidized for 5 min. A : 200 reflection of alloy matrix, I : 211 reflection of In_2O_3.

Table 2. Comparison of the observed lattice spacings and intensities of the reflections obtained from Fig.1 with those of the reference substances.

Observed values		Reference substances measured by X-rays					
		Alloy			ASTM card		
					In_2O_3		
dA	I	dA	I/I_1	hkl	dA	I/I_1	hkl
4.24	m				4.13	14	211
2.97	s				2.921	100	222
2.55	w				2.529	30	400
2.38	m	2.322	100	111	2.385	8	411
2.18	m				2.157	6	332
2.04	m	2.014	52	200			
					1.984	10	431
					1.848	4	521
1.80	s				1.788	35	440
					1.735	4	530, 433
					1.641	6	611
					1.561	4	541
1.55	w				1.525	25	622
1.50	w				1.492	6	631
1.45	vw	1.427	32	220	1.460	6	444

Table 3. Comparison of the observed lattice spacings and intensities of the reflections obtained from Fig.2 with those of the reference substances.

Observed values		Reference substances measured by X-rays								
		Alloy			ASTM cards					
					In_2O_3			SnO_2		
dA	I	dA	I/I_1	hkl	dA	I/I_1	hkl	dA	I/I_1	hkl
4.06	m				4.13	14	211			
								3.351	100	110
2.87	s				2.921	100	222			
								2.644	81	101
2.50	m				2.529	30	400			
2.36	vvw	2.322	100	111	2.385	8	411	2.369	24	200
								2.309	5	111
2.14	m				2.157	6	332			
2.03	vvw	2.014	52	200						
1.98	m				1.984	10	431			
					1.848	4	521			
1.78	s				1.788	35	440	1.765	63	211
					1.735	4	530, 433			
1.63	w				1.641	6	611	1.675	63	220
					1.561	4	541	1.593	8	002
1.53	m				1.525	25	622			
					1.492	6	631	1.498	13	310
1.42	vvw	1.427	32	220	1.460	6	444	1.439	17	112

Figure 3 was obtained from Alloy No.3, the same alloy as in Fig.2, now oxidized for 20 min. The lattice spacings are shown in Table 4, revealing 110 and 101 reflections of SnO_2 in addition to those of the alloy matrix and In_2O_3. A similar diffraction pattern was obtained from the specimen oxidized for 60 min, showing that the detection of SnO_2 on the oxidized surface depends on the oxidation time.

Figure 4 was obtained from Alloy No.4 oxidized for 30 sec, and the observed lattice spacings are shown in Table 5. The diffraction pattern shows reflections from three kinds of crystals: Alloy matrix, In_2O_3, and SnO_2. In the diffraction pattern, the rings having very bright parts correspond to the reflection from the In_2O_3. When the Sn content increases up to 0.9 wt%, the reflections from SnO_2 appear at the very short oxidation time of 30 sec.

It may be concluded that the oxides on the oxidized alloy surface depend on the concentrations of In and Sn as well as on the oxidation time. The experimental results are summarized in Fig.5, here the curved line divides the region with only alloy matrix and In_2O_3 from that with alloy matrix, In_2O_3, and SnO_2. In Alloy No.6 containing only Sn, the diffraction is from only SnO_2, and not from the alloy matrix, indicating that the alloy surface is covered by a uniform SnO_2 layer. The diffraction from the alloy matrix appears when adding trace amounts of In.

Figure 6 shows secondary electron images, obtained from the oxidized surface of Alloy No.3 at four oxidation times. The topography of the surface changes with oxidation time : Many minute holes are observed at 30 sec(a) and the hole size and roughness of the surface increases at 5 min(b). For the longer oxidation times, 20 min(c) and 60 min(d), the roughness increases further.

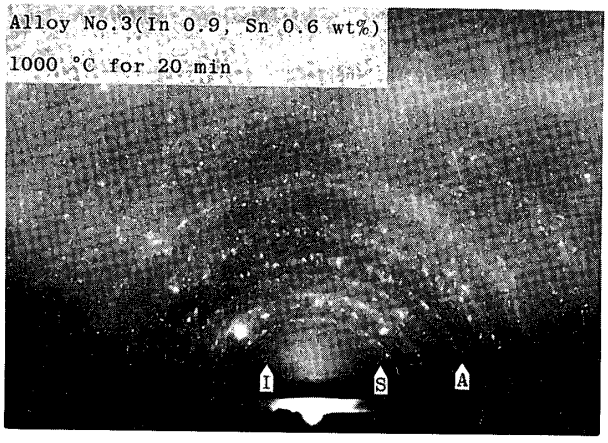

Fig. 3 Reflection high energy electron diffraction pattern from the surface of Alloy No.3, oxidized for 20 min. A : 200 reflection of alloy matrix, I: 211 reflection of In_2O_3, S : 110 reflection of SnO_2.

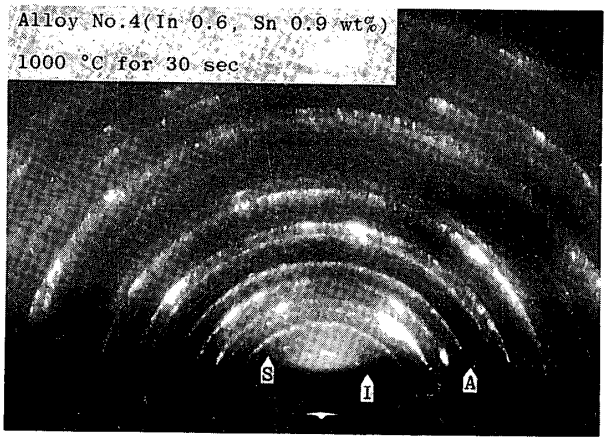

Fig. 4 Reflection high energy electron diffraction pattern from the surface of Alloy No.4, oxidized for 30 sec. A : 200 reflection of alloy matrix, I : 211 reflection of In_2O_3, S : 110 reflection of SnO_2.

Table 4. Comparison of the observed lattice spacings and intensities of the reflections obtained from Fig.3 with those of the reference substances.

Observed values		Reference substances measured by X-rays								
		Alloy			ASTM cards					
					In_2O_3			SnO_2		
dA	I	dA	I/I_1	hkl	dA	I/I_1	hkl	dA	I/I_1	hkl
4.21	vw				4.13	14	211			
3.35	vw							3.351	100	110
2.91	s				2.921	100	222			
2.67	vvw							2.644	81	101
2.54	m				2.529	30	400			
2.33	s	2.322	100	111	2.385	8	411	2.369	24	200
								2.309	5	111
2.14	w				2.157	6	332			
2.01	m	2.014	52	200						
					1.984	10	431			
1.87	vvw				1.848	4	521			
1.79	m				1.788	35	440	1.765	63	211
					1.735	4	{530 433			
1.64	w				1.641	6	611	1.675	63	220
					1.561	4	541	1.593	8	002
1.52	m				1.525	25	622			
					1.492	6	631	1.498	13	310
1.44	w	1.427	32	220	1.460	6	444	1.439	17	112

Table 5. Comparison of the observed lattice spacings and intensities of the reflections obtained from Fig.4 with those of the reference substances.

Observed values		Reference substances measured by X-rays								
		Alloy			ASTM cards					
					In_2O_3			SnO_2		
dA	I	dA	I/I_1	hkl	dA	I/I_1	hkl	dA	I/I_1	hkl
4.22	w				4.13	14	211			
3.41	vvw							3.351	100	110
2.97	s				2.921	100	222			
2.70	vvw							2.644	81	101
2.57	m				2.529	30	400			
2.37	s	2.322	100	111	2.385	8	411	2.369	24	200
								2.309	5	111
2.18	w				2.157	6	332			
2.05	s	2.014	52	200						
					1.984	10	431			
1.82	s				1.848	4	521			
					1.788	35	440	1.765	63	211
					1.735	4	{530 433			
1.67	w				1.641	6	611	1.675	63	220
1.58	vvw				1.561	4	541	1.593	8	002
1.54	m				1.525	25	622			
					1.492	6	631	1.498	13	310
1.45	s	1.427	32	220	1.460	6	444	1.439	17	112

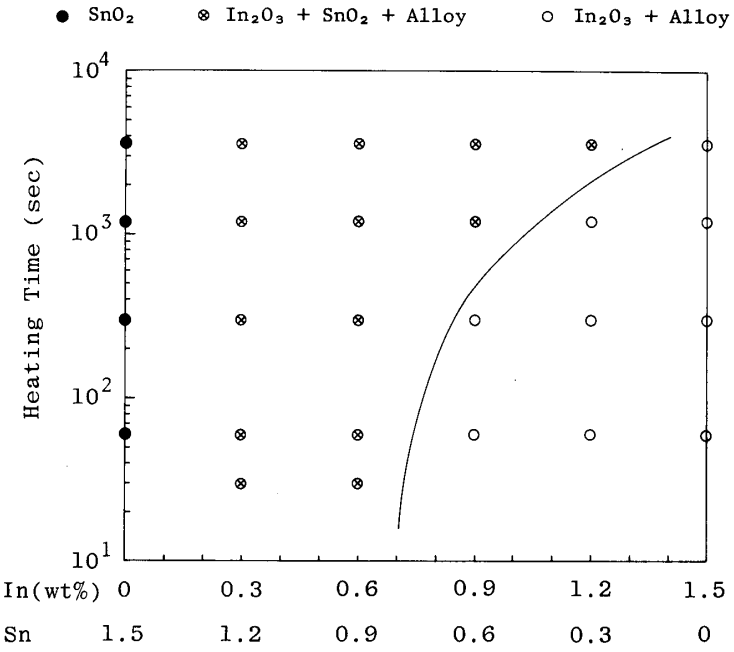

Fig. 5 Relationship between the heating times in air and the concentrations of In and Sn for the substances on the oxidized surface.

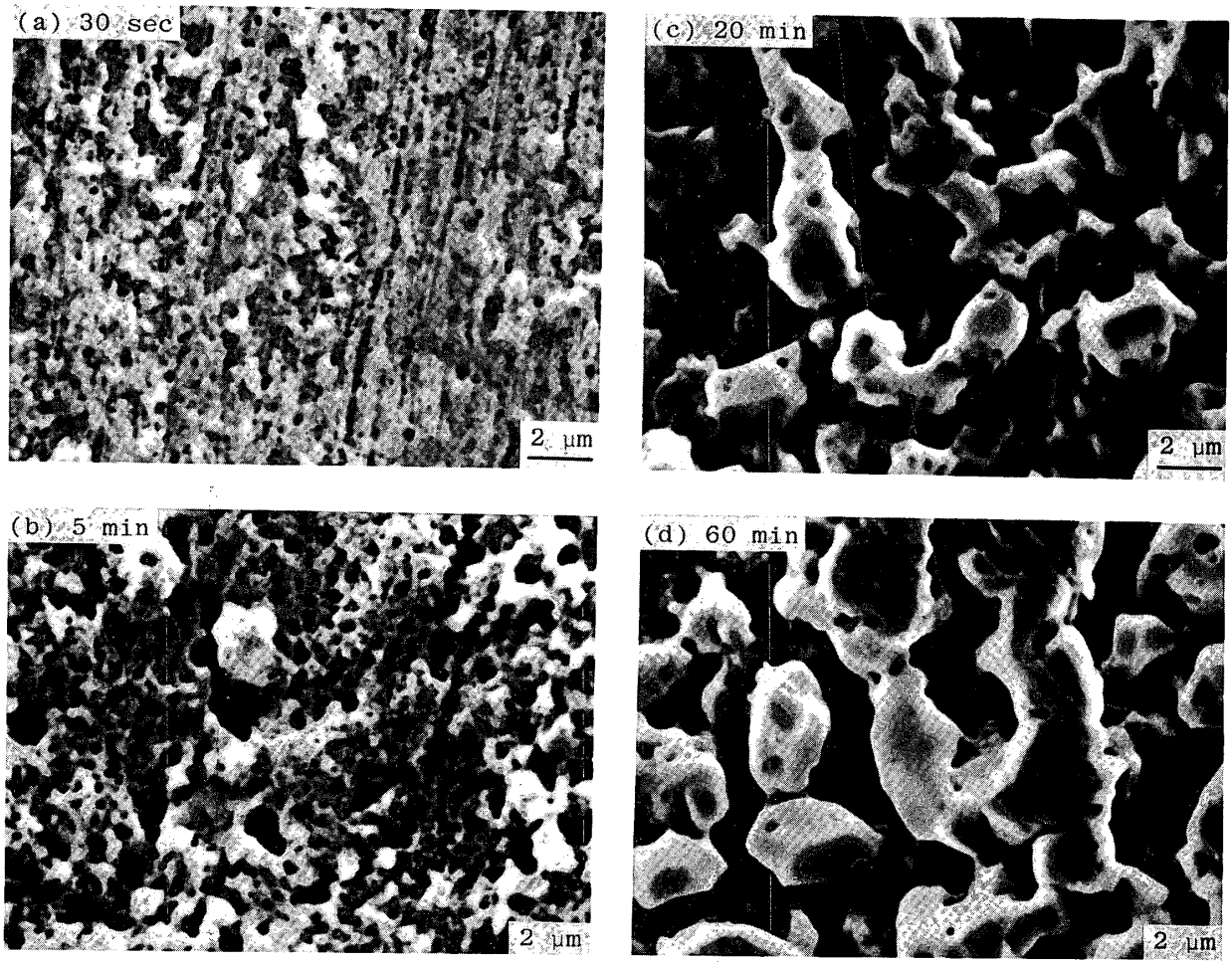

Fig. 6 Secondary electron images with oxidation times, obtained from the oxidized surface of Alloy No.3.

Discussion

No uniform oxide layer on the alloy surface

The diffraction rings from the alloy matrix by reflection electron diffraction (Fig .1, Fig. 2, Fig.3, and Fig.4) gives evidence of the exposure of the alloy matrix, demonstrating the non-existence of a uniform oxide layer of In_2O_3 and SnO_2 thicker than 100 Å. It has been reported that with XMA there is no external oxide layer,[10] and this result is confirmed by the reflection electron diffraction. Based on XMA is has been suggested that the convex parts observed in Fig.6(d) are the alloy itself[10] ; the massive convex parts may be explained as single crystals that become larger by agglomeration with longer oxidation times, resulting in the spotty diffraction rings appearing with increased oxidation times as shown in Fig.1 and Fig.3. An explanation for the absence of a uniform oxide layer may be that oxidation proceeds as internal oxidation, precipitating preferentially formed oxides at grain boundaries by the diffusion of O^{2-} ions through the In_2O_3.[10]

Alloy No.3 containing 0.9 wt% In and 0.6 wt% Sn has a composition near one of the commercial gold alloys for porcelain-metal bonding.[9] The influence of the exposure of the surface of the alloy matrix on the bonding strength between porcelain and metal is not clear. The increased roughness of the oxidized surface due to high temperature oxidation as shown in Fig.6 may increase the bonding strength by a mechanical bonding effect.

Preferential oxidation of In

For a metal to oxidize preferentially it would be expected that the formed M_UO_V oxide has the larger Gibbs standard free energy of formation ($-\Delta G$), higher concentration, and bigger metal/oxygen atomic ratio, u/v.[12] Both the value of $-\Delta G$ (In_2O_3 : 82.1 Kcal, SnO_2 : 74.9 Kcal at 1000 ℃)[13] and u/v (In_2O_3 : 2/3, SnO_2 : 1/2) for In_2O_3 are higher than for SnO_2, and In may be expected to oxidize preferentially. This was supported by the results, In_2O_3 predominated on the alloy surface in a wide composition range.

When the structure of the oxidation zones on the alloy surface changes in the depth direction, different analytical methods give different results as a method has a characteristic analytical region, both across and into the specimen surface. Figure 7 shows the results of X-ray diffraction, obtained from a plate specimen of Alloy No. 3 oxidized at 1000 ℃ for 5 min. Compared with the predominant In_2O_3 the diffraction lines of SnO_2 appear only weakly. For the reflection electron diffraction, SnO_2 rings were not observed (Fig. 2, Table 3) for the same specimen. It has been reported that In_2O_3 enriches on the surface and SnO_2 enriches in the inner part below 1 μm to 2 μm.[9,10] The different results obtained by the two analytical methods are explained by the different diffraction depths ; X-rays diffract from regions below 1 μm, while electrons diffract only from the top layer down to several hundred Å.

For high Sn contents, the top surface is resolved by reflection electron diffraction to be

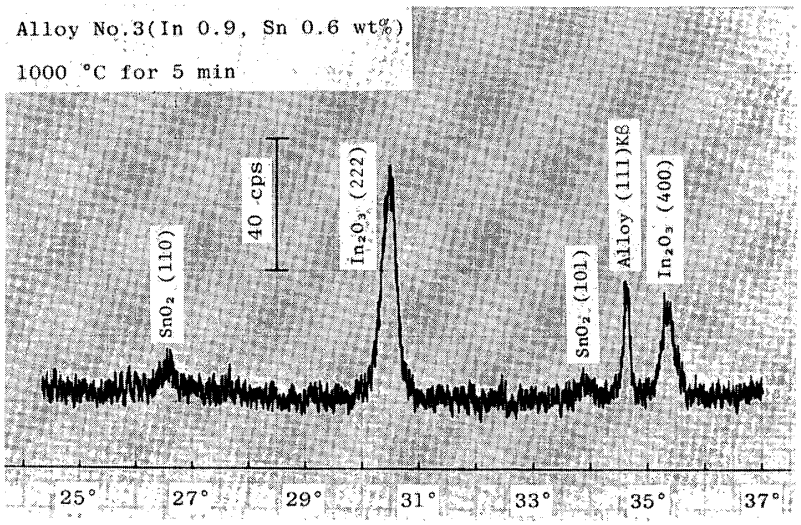

Fig. 7 Results of X-ray diffraction obtained from plate specimen of Alloy No. 3, oxidized for 5 min.

composed of a mixture of alloy matrix, In_2O_3, and SnO_2 ; while at low Sn contents and short oxidation times it consists of a mixture of alloy matrix and In_2O_3. The state of the top surface of the gold alloys is influenced by In and Sn contents, and oxidation time ; the main factor determining the state of the surface is the preferential oxidation of In.

Conclusions

In the present study, the top surface of gold alloys containing small amounts of In and Sn for porcelain bonding, oxidized at 1000 ℃ in air, was investigated by reflection high energy electron diffraction in order to obtain data to clarify the reaction process and the porcelain-gold alloy bonding mechanism.

In the range that can be detected by reflection electron diffraction, the oxidized alloy surface is not covered with a uniform oxide layer. The alloy itself is partially exposed for alloy containing both In and Sn, or only In, oxidized for 30 sec to 60 min. The roughness of the oxidized surface formed by high temperature oxidation increases with longer oxidation times and this may play a role in increasing the mechanical bonding strength between porcelain and metal. However, effects of the exposure of the alloy matrix on the bonding strength is not clear in the present study.

The oxides formed by high temperature oxidation on the surface are In_2O_3 and SnO_2. In_2O_3 rather than SnO_2 is preferentially formed. When the Sn content is less than 0.6 wt%, SnO_2 can not be detected by reflection electron diffraction at short oxidation times. The oxides on the surface depend on both the concentrations of In and Sn, and the oxidation times.

Acknowledgments

This work has been partially supported by the fund for the promotion of science at Higashi-Nippon-Gakuen University.

The authors wish to thank Prof. M. Ohta and Dr. S. Ohkawa (Hokkaido Univ.) for the use of the electron probe X-ray microanalyser and Mr. T. Kannari (Higashi-Nippon-Gakuen Univ.) for his assistance in the reflection electron diffraction experiments.

References

1. Ohno, H., Ichikawa, T., Shiokawa, N., Ino, S., and Iwasaki, H. : ESCA Study on the Mechanism of Adherence of Metal to Silica Glass, J. Mat. Sci., 16(5);1381-1390, 1981.
2. Lautenschlager, E.P., Greener, E.H., and Elking, W.E. : Microprobe Analysis of Gold-Porcelain Bonding, J. Dent. Res., 48(6);1209-1210, 1969.
3. Cascone, P.J. and Tuccillo, J.F. : Theoretical Interfacial Reactions Responsible for Bonding in Porcelain-to-Metal Systems (Part I), IADR Prog. & Abstr., 56, No.640, 1977.
4. Cascone, P.J., Massimo, M., and Tuccillo, J.F. : Theoretical Interfacial Reactions Responsible for Bonding in Porcelain-to-Metal Systems (Part II), IADR Prog. & Abstr., 57, No.872, 1977.
5. Ringle, R.R., Fairhurst, C.W., and Anusavice, K.J. : Microstructures in Non-precious Alloy Near the Porcelain-Metal Interaction Zone, J.Dent.Res., 58(10);1987-1997, 1979.
6. Yli-Urpo, A. : Investigation of a Dental Gold Alloy and its Ceramic Bonding, Acta.Odont.Scand. Suppl., 69; 59-182, 1975.
7. King, B.W., Tripp, H.P., and Duckworth, W.H. : Nature of Adherence of Porcelain Enamels to Metals, J. Amer.Ceram.Soc., 42(11);504-525, 1959.
8. Clark, D.E., Pantano, C.G., and Onoda, G.Y. : Auger Analysis of Brass-Enamel and Stainless Steel Enamel Interfaces, J.Amer.Ceram.Soc., 58(7-8);336-337, 1975.
9. Ohno, H., Miyakawa, O., Watanabe, K., and Shiokawa, N. : The Structure of Oxide Formed by High-temperature Oxidation of Commercial Gold Alloys for Porcelain-Metal Bonding, J.Dent.Res., 61(11);1255-1261,1982.
10. Ohno, H., Kanzawa, Y., Kawashima, I., and Shiokawa, N. : Structure of High Temperature Oxidation Zones of Gold Alloys for Metal-Porcelain Bonding Containing Small Amounts of In and Sn, J.Dent.Res., in press.
11. Hirsch, P.B., Howie, A., Nicholson, R.B., Pashley, D.W., and Whelan, M.J. : Electron Microscopy of Thin Crystals, 90-91, Butterworths, London, 1965.
12. Igarashi, T., Shibata, M., and Kodama, Y. : The Precipitaion Behavior of Oxide during Internal Oxidation of Ag-Sn Alloys, J.Jpn.Inst.Met., 44(4);378-386, 1980.
13. Kubschewski, O. and Alcock, C.B. : Metallurgical Thermochemistry, 5th ed., 378, Pergamon Press, New York, 1979.

陶材と金属の溶着機構の解明に関する基礎的研究
－反射電子回折による金合金の酸化表面の解析－

大野　弘機，神澤　康夫，川島　　功，山根　由朗，鷹觜　聖子

東日本学園大学歯学部歯科理工学講座
（主任：神澤　康夫教授）

抄　　録

陶材焼付用合金の合金表面を解析することは，その面が溶融した陶材と接するので，両者の界面反応と溶着機構を解明するために必要である。本研究は，卑金属成分として，InとSnを総量1.5wt％含む金合金を，1000℃で30sec-60min間，大気中で加熱し，酸化物など，表面状態の変化について，反射電子回折で解析した。Snのみを添加した合金を除いて，それ以外の合金では，一様な酸化皮膜は形成されず合金そのものが部分的に露出している。生成した酸化物は，In_2O_3とSnO_2で，In_2O_3が広い組成範囲で優先的に形成される。SnO_2は，Snが0.6wt％以下で，短時間の加熱では，回折リングが観察されないが，長時間の加熱になると観察されるようになる。酸化物の状態に対して加熱時間と卑金属成分濃度の依存性が認められる。高温酸化で生じた表面の凹凸は，加熱時間が増すに伴って増加する。これによって，陶材と合金の機械的結合の向上を期待できるが，合金そのものが露出していることの焼付機構への寄与は不明である。

受付：昭和57年10月12日
本論文の要旨は第1回日本歯科理工学会(昭和57年4月3日)において発表した。